Developmental Biology **216,** 457–468 (1999)
Article ID dbio.1999.9500, available online at http://www.idealibrary.com on IDEAL®

A Three-Dimensional Model of the Mouse at Embryonic Day 9

R. M. Brune,*[,1] J. B. L. Bard,* C. Dubreuil,† E. Guest,† W. Hill,† M. Kaufman,* M. Stark,† D. Davidson,† and R. A. Baldock†

**Anatomy Section, Biomedical Sciences, University of Edinburgh, Teviot Place, Edinburgh, EH8 9AG, United Kingdom; and †MRC Human Genetics Unit, Western General Hospital, Crewe Road, Edinburgh, EH4 2XU, United Kingdom*

This paper describes a digital, three-dimensional model of the mouse embryo at E9. The model was made by reconstruction from images of serial histological sections digitally warped to remove distortions and has a resolution of approximately 9 μm. The model can be digitally resectioned in any plane to provide images which resemble conventional histological sections. The main tissues have been identified and delineated by digital painting so that the anatomical components can be visualized and manipulated in 3-D surface- and volume-rendered views. This provides a three-dimensional definition of anatomy that will provide a useful tool for interpreting and understanding spatial data in mouse embryos. The anatomy of the model is discussed where it provides landmarks for interpretation and navigation or where it is unexpected in light of existing descriptions of the E9 mouse embryo. The complete anatomy is not presented in this paper but will be available on CD-ROM. A detailed description of the technical aspects of the construction of the model is included in an appendix. The model is the first of a series that will form the basis for an atlas/database of mouse development. This reconstruction and its associated anatomy are available in a variety of data formats with some supporting software from http://genex.hgu.mrc.ac.uk/. **© 1999 Academic Press**

Key Words: **E9 mouse embryo; Theiler stage 14; atlas; anatomy; 3-D reconstruction; voxel images; anatomical nomenclature.**

INTRODUCTION

The mouse is the major model system for studying the genetic basis of mammalian development, yet there is no detailed, systematic reference description of the morphological phenotype of the mouse embryo. Such a description is necessary to help us analyze the vast amount of data needed to understand gene function. The description should provide a common framework in which to map and compare data on cell activities, gene expression patterns, mutant phenotypes, etc. A key aspect of these data is that much of it is essentially spatial and does not necessarily follow tissue boundaries; the framework must therefore accommodate spatially mapped data as well as information assigned to named parts of anatomy. In order to permit an understanding of tissue dynamics and morphogenesis, such a framework should combine an overview of the three-dimensional morphology of organs and tissues with an indication of their histological structure and the distribution of cells. Conventional embryo atlases (Rugh, 1968; Theiler, 1989; Kaufman, 1992) can only provide a limited number of pictures and section planes. A more complete description of mouse anatomy that not only details the anatomical structures, but can also be viewed in any arbitrary orientation or plane of section, is now necessary.

To provide such a description, we are creating 3-D digital voxel[2] models of mouse embryos from images of serial histological sections. We have based the models on conventional histological sections, rather than, e.g., MR images, to provide a view of the material that is familiar to developmental biologists. To relate this purely spatial description to anatomy, we have delineated the boundaries of structures that are recognizable with standard staining and that

[1] To whom correspondence should be addressed. E-mail: R.Brune@ed.ac.uk.

[2] Voxel is the 3-D equivalent of pixel in a 2-D image which is the picture element representing the image content at that point. In this case the voxels are arranged on a rectangular 3-D grid.

0012-1606/99 $30.00
Copyright © 1999 by Academic Press
All rights of reproduction in any form reserved.

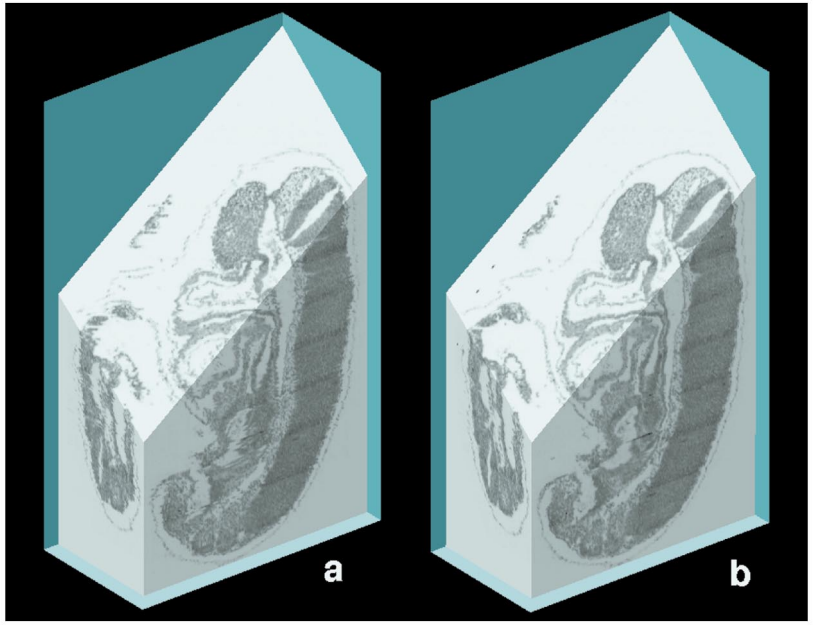

1

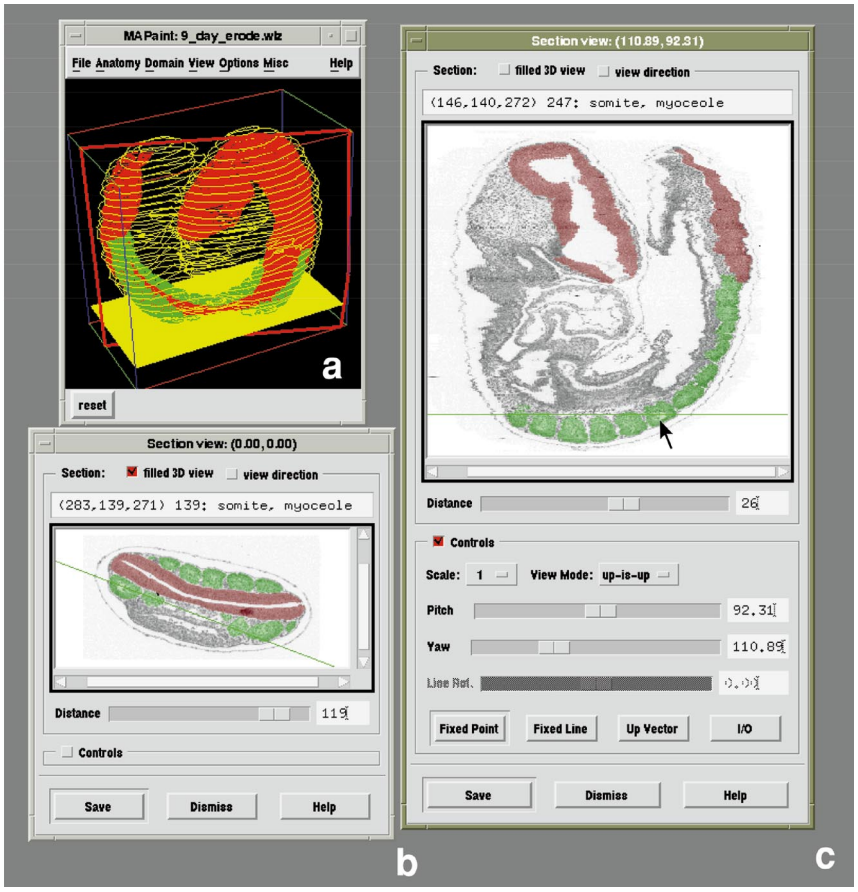

2

FIG. 1. Two views of the E9 mouse embryo reconstructed from tissue sections, and displayed as "cut-blocks," with each showing two planes orthogonal to the original sections and one arbitrary plane: (a) has only had the sections registered, while (b) has been registered and warped. The effect of warping can be most easily observed by comparing the peripheral membranes of the heart and of the amnion enclosing the embryo.

FIG. 2. Screen shot of MAPaint showing two arbitrary section views of the histology with a number of painted domains (b, c) and a 3-D feedback and navigation window (a). The orientation controls for one of the planes (c) are shown and give the user complete control of the section position, orientation and screen display (including left–right inversion). The intersection of each view with the other is designated by a green line. As the cursor is passed over the section image the underlying anatomical component is displayed on the status line (above the image). The 3-D feedback window will show the current domains as a simplified 3-D view which can be arbitrarily rotated and scaled. The section views appear as optionally filled outlines on the 3-D view (yellow plane (b), red plane (c)) and can be used to select sections relative to 3-D features.

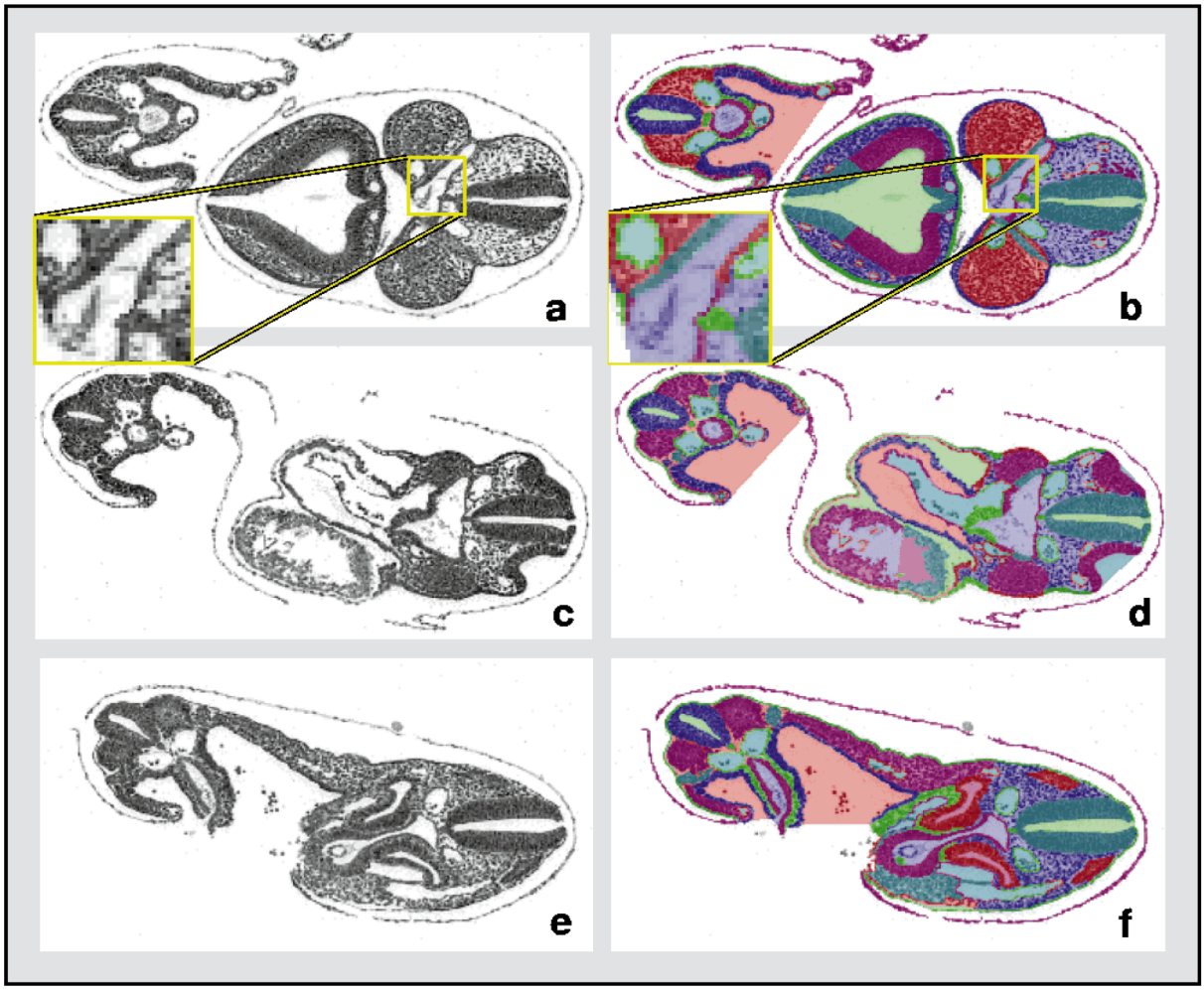

FIG. 3. Three representative sections: (a) through the forebrain, in the region of the optic vesicles; through the first branchial arches, one shown on either side of the remnants of the buccopharyngeal membrane in the region of the oral pit; and the hindbrain (shown in the right side of the section). This section is also through the proximal part of the tail (top left of the section). (c) Through the thoracic region, displaying the primitive ventricle, bulbus cordis and outflow tract of the primitive heart; in the dorsal region of the embryo, the left otic pit is clearly seen. (e) Through the caudal region of the foregut, close to the foregut–midgut junction; the rostral part of the septum transversum is seen to be surrounding the hepatic diverticulum; the somites, located on either side of the tail region, are also clearly seen (Kaufman, 1992, plates 18a and 18b). Toward the bottom right of section (a), a magnified area of the rostral part of the first pharyngeal pouch is shown, and the same area painted is shown in (b). In the complementary "painted" sections, b, d, and f, the anatomical domains in each of these sections have been displayed using only five colors (it was not possible to give every tissue its own color and view the underlying histology).

are named in the standard anatomy database (Bard *et al.*, 1998). These models will form the framework for one or more databases in which any spatially organized data, e.g., gene expression, can be mapped[3] (Baldock *et al.*, 1992; Davidson and Baldock, 1997; Davidson *et al.*, 1997). These data can then be analyzed, compared, and interrogated in purely spatial terms as well as in relation to the underlying anatomy. The standard anatomical nomenclature, digital embryos, and gene-expression database are being developed as part of the Mouse Gene Expression Information Resource[4] (MGEIR, Ringwald *et al.*, 1994).

In this paper we report the first digital model of the E9 (9 dpc, Theiler stage 14) mouse embryo which is now available on CD-ROM. The model can be digitally resectioned in any arbitrary plane to show a histological section that corresponds to a section through the user's own material, with

[3] See http://genex.hgu.mrc.ac.uk/SamplePics/#Gene Expression.

[4] See our WWW site: http://genex.hgu.mrc.ac.uk.

Copyright © 1999 by Academic Press. All rights of reproduction in any form reserved.

the advantage that all the tissues are delineated and named. Such a model can also be displayed in a volume-rendered format, the digital equivalent of a whole-mount embryo preparation. This provides a useful tool for relating any spatial data to anatomy and also as a teaching aid (Kaufman *et al.*, 1996). We discuss the anatomy of the model where it is unexpected in light of existing descriptions of E9 mouse anatomy for purposes of presenting the advantages of the system and aiding the user to navigate through the model with the help of morphological landmarks.

The E9 embryo was chosen for our initial model because it is intermediate in complexity and therefore provides a good test of our approach and also because it represents an important period in development at the transition between embryogenesis and organogenesis. To ensure consistency of reference material we have used serial sections from the E9 embryo illustrated in the "Atlas of Mouse Development" (Kaufman, 1992) which is typical of this stage.

MATERIAL AND METHODS

Embryos

The E9 embryo used for the model was obtained by mating a (C57BL×CBA)F1 hybrid male with a female of the same genetic constitution. Preparation of the embryo has already been described (Kaufman, 1992): in summary, the embryo was dissected free of its extraembryonic membranes (except amnion), fixed in Bouin's fixative, routinely processed and embedded in wax, and then sectioned at a nominal thickness of 7 μm. Contiguous ribbons of sections were collected, ordered, and mounted on glass slides and then stained with hematoxylin and counterstained with eosin.

Reconstruction

The gray-level (i.e., photographic) voxel model was reconstructed using the full set of 307 histological sections. The requirement was to produce a 3-D model representative of the E9 mouse embryo that can be used for resectioning at arbitrary orientations to allow mapping of gene-expression data. For this purpose we have developed a technique that produces a reconstruction from a set of section images without fiducial marks for registration. The digital embryo does not, therefore, necessarily have exactly the same shape as the original specimen but has had the random distortions arising from the sectioning process largely removed. The overall alignment of the sections was established by demanding that the external shape of the final reconstruction be representative of a fixed embryo of this stage. The details of the process are given in the appendix and the result for the E9 embryo is shown in Fig. 1.

Delineating Anatomical Structures

Anatomical structures were delineated using a program (MAPaint) developed for this purpose. This software includes some automatic functions (e.g., edge detection), but, for the model described here, we found that much of the delineation had to be done manually. At any one time, MAPaint allows the user to delineate up to 32 structures in any arbitrary view (Fig. 2). The anatomical domains are stored as separate 3-D binary images in the database and there is no limit, in principle, on how many domains can be delineated and independently stored.

Our intention has been to delineate the boundaries of all the major tissues and their constituent parts that can be recognized in this embryo, not to paint individual cells. Tissues were painted serially, mostly on images of the original transverse sections, but with the help of other planes of sectioning where necessary. In all cases, tissue boundaries were established by checking the morphology of the original sections using a microscope. The delineated boundaries where subsequently checked and corrected if the error was greater than one pixel.

While most intertissue boundaries could be identified through inspection of the original section, a few had to be determined on the basis of reconstructed planes (e.g., the somites) or had to be determined arbitrarily. In some cases, there was no discontinuity in tissue structure in passing from one component to another (e.g., where the branchial pouches or endodermal linings of the branchial arches meet the anterior foregut); in such cases, the standard approach was to mark the boundary on the basis of its 3-D morphology or its position relative to other tissues (see Figs. 3a–3d). A further problem arose in delineating partially formed structures (e.g., in defining a boundary between the prenotochordal mesenchyme and the condensed notochord) where the decision must be arbitrary, as there is a developmental transition zone rather than a true boundary. In other cases, boundaries were difficult to define because they were not clearly indicated by the staining (e.g., that between the common atrium and the primitive ventricle). Where a boundary was not clearly defined morphologically on a single section, it was placed according to one or more of the following of criteria: (i) 3-D morphology, (ii) position of surrounding tissues, (iii) cell arrangement, or (iv) by selecting a boundary half way between positions where the tissue identification is clear. In instances where the placement of a boundary involved informed judgment or arbitrary decision, the basis for placement has been recorded in notes on the CD-ROM.

Visualization

We have used three methods to visualize the gray-level image and its delineated anatomy:

- Arbitrary digital histological sections through the volume of the 3-D model using MAPaint;
- "Whole-mount" 3-D visualization viewed by direct volume-rendering techniques; and
- 3-D visualization of components as surfaces with controllable properties such as color and transparency (including true stereo viewing with appropriate hardware).

Digital sections. MAPaint (Fig. 2) provides an interface for displaying (and modifying) 3-D domains in the embryo model. The program allows the user to view any number of 2-D sections through the model, each of which can be set at any viewing angle. To assist navigation, it is possible to set either one or two fixed or fiducial points in the model about which the viewed section will rotate. When the appropriate angle has been set, the interface provides a "slider" control to allow the user to pan through the set of parallel sections in that orientation with feedback provided in a 3-D navigation window. The required reconstruction is read from the Mouse Atlas CD-ROM, and the user is provided with a 3-D outline view of the embryo and an anatomy "menu" which allows any of the predefined domains to be read in and visualized. The

Copyright © 1999 by Academic Press. All rights of reproduction in any form reserved.

anatomy menu matches the structure of the E9 anatomy hierarchy defined in the online database (Bard *et al.*, 1998).

Within the program, anatomical domains can be shown either as transparent or as solid overlays over the gray-level histology image and each viewing window provides feedback of the current tissue under the screen pointer. An example of the use of MAPaint to view structures is shown in Fig. 2. MAPaint was written in C using X11/Motif, will run on almost any UNIX-based workstation and is available for use with the CD-ROM.

3-D volume rendering. For volume rendering we have used the "Visualisation Toolkit" (VTK, Schroeder *et al.*, 1998) to display views of the "painted" volume from MAPaint. This allows each tissue to be displayed in a different color to show the positions of tissues in whole-mount preparations. Arbitrary domains defined using MAPaint can be visualized in this way. Figure 4 shows two renderings of the embryo: the first is the histology alone and the second shows a number of tissues in different colors; these could be used, e.g., as landmarks to aid orientation and location.

3-D surface rendering. We have used the AVS visualization system (Advanced Visual Systems Inc., U.S.A.) to provide surface rendered 3-D view of the structure of the anatomical domains. We have used the AVS modules to convert the 3-D voxel-based domains to a triangulated surface which can then be viewed in the "geometry viewer." This allows interactive manipulation of the viewing parameters of each surface including orientation, scale, color, lighting, reflection properties, transparency, and shading. For this work, we used a Silicon Graphics Indigo 2 with 128 Mbyte RAM and Extreme graphics which allows almost real-time manipulation of the viewed data. This workstation also allows the use of "Crystal Eyes" stereo glasses (StereoGraphics Corporation, U.S.A.) in which two views of the data differing by a small viewing angle are presented to each eye independently. This results in a clear 3-D view of the structures with no loss of colors or other viewing parameters. Figures 5–7 show some examples of the 3-D rendering that can be provided by the AVS software.

RESULTS

The Model Embryo

The digital embryo can be displayed as if in a 3-D paraffin block, "trimmed" to demonstrate a selection of planes of section that show some of the histology (Fig. 1b). Two-dimensional section images in the plane of the original histological sections show the resolution of the histology and anatomical delineation in the 3-D model. In other, arbitrary, planes of section the resolution is slightly lower since the maximum dimension within a pixel is 9 μm (diagonal of a $4 \times 4 \times 7$-μm voxel). This resolution is still adequate, however, to discern the morphology and boundaries of most tissues. As for the anatomical resolution, the smallest tissue that was delineated is the biliary bud, an approximately globular structure with a diameter of $\sim$35 μm; the thinnest tissue is the walls of the blood vessels, at only one pixel (4 μm) thick. For some purposes a higher resolution may be important; therefore, the original image of the sections, with a pixel size of 1.36 μm, is provided for reference on the CD-ROM.

Three-dimensional volume rendering gives the appearance of a whole-mount preparation and illustrates the level of realism achieved by the model (Fig. 4). It is worth noting that individual tissues and their spatial relationships are most clearly discerned when the 3-D volume rendered model is viewed while rotating (e.g., using AVS). The external appearance of the model embryo is normal and there seems to be little evidence of shrinkage. There is, for example, no sign of somites bulging through the surface epithelium, an artifact often detected when fixed material is prepared for SEM. Figure 5a shows a 3-D view of the outline of the embryo with its amnion removed. The embryo has almost completed the process of turning: the right-hand somites, dorsal aorta, and umbilical vein and the right side of the mesothelial lining of the intraembryonic coelom are located more ventrally than those on the left (Figs. 5b and 5c), and the septum transversum (Fig. 7) is situated to the left.

Several other external features confirm that this reconstruction conforms with the standard description of the E9 embryo. The first two branchial arches are present, the first having no clear line of demarcation between its maxillary and mandibular components, the otic placode has indented to form the otic pit, and the forelimb bud is only just beginning to form. The cephalic part of the neural tube has closed, although the caudal neuropore is still open. There is still evidence of a primitive streak, but the primitive groove is no longer present. The degree of curvature of the craniocaudal axis accords with the standard descriptions for the stage (Theiler, 1972; Kaufman, 1992). The internal organization of this embryo also matches that originally described and analyzed by Theiler (1972) for this stage: there are 17 somites, the nephrogenic cord, nephric duct (Fig. 5c), Rathke's pouch and the hepatic diverticulum with its biliary bud have all formed, and the buccopharyngeal membrane has recently ruptured (Fig. 7).

The only apparently unusual feature noted in the model embryo is a twist in the caudal tip of the future spinal cord. Although this feature seems not to have been described in the literature, it may not reflect any abnormality, as of 29 E9 embryos (same F2 cross) examined, 14 showed this feature.

Anatomical domains. Table 1 lists the anatomical components that were identified in the original histological sections and delineated in the reconstruction. It should be noted that this embryo represents a single time point during the interval defined by E9 and thus contains only a subset of the components listed in the standard nomenclature for the stage as a whole (some form or disappear during this period). Some tissues named in the anatomical database cannot be resolved or distinguished at the resolution of the reconstruction and are not individually represented by painted domains. For example neural-crest-derived cells cannot be distinguished morphologically from those derived from mesoderm without the use of specific markers.

Copyright © 1999 by Academic Press. All rights of reproduction in any form reserved.

4

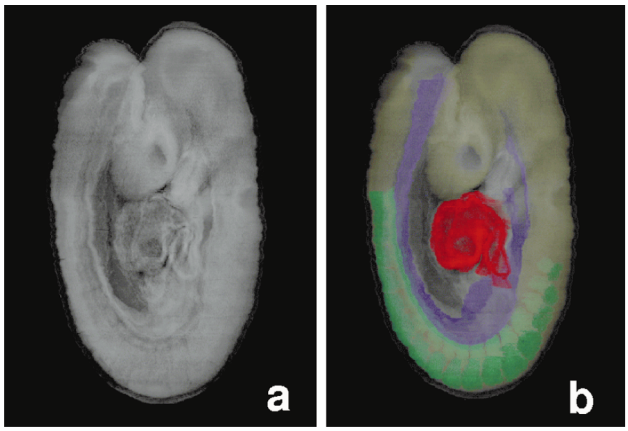

5

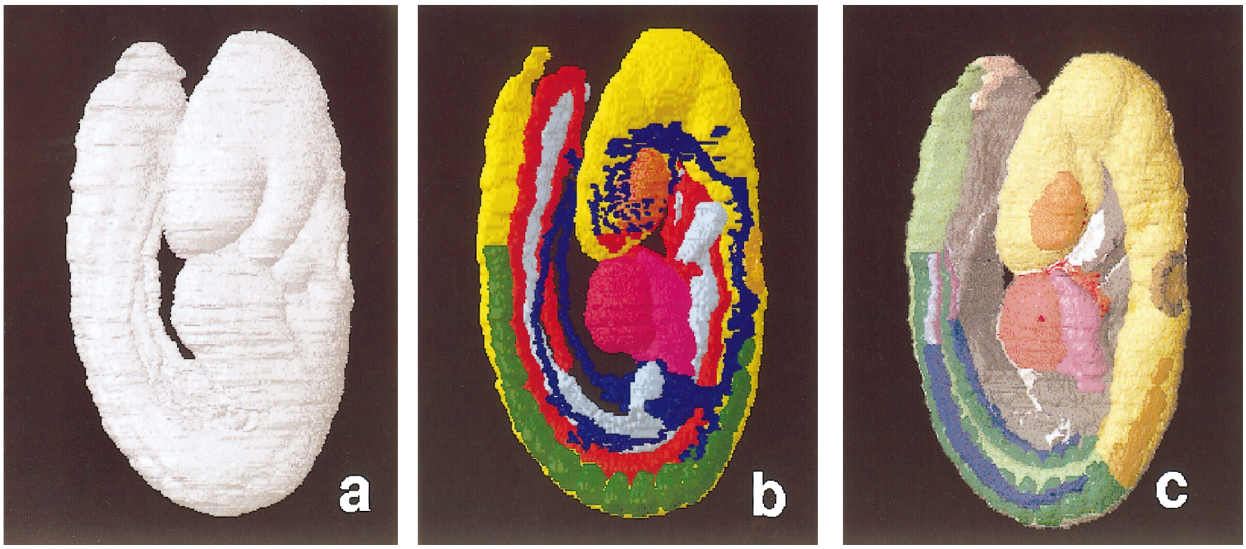

FIG. 4. Volume rendered views of the E9 embryo. (a) A whole-mount view of the E9 reconstruction from histology; (b) as (a) but with heart, somites, neural tissue, and gut colored to act as landmarks.

FIG. 5. 3-D views of the E9 reconstruction with the amnion removed: (a) outline of the embryo; (b) neural tissue (yellow), optic vesicles (orange), otic pit (pale orange), somites (dark green), arteries (orange red), veins (dark blue), heart [common atrial chamber (lilac), primitive ventricle (magenta), bulbus cordis, and outflow tract (red)] and gut (light blue); (c) future brain (yellow), optic vesicles (orange), future spinal cord (lime green), head somites (dark yellow), body somites (dark green), heart (see b), intermediate mesenchyme (dark blue), nephrogenic cord (purple), presumptive nephric duct (light lilac), and primitive streak (light pink) in a translucent white outline of the embryo.

Anatomical Relationships

Landmarks. The painted anatomical components provide a number of landmarks by which someone with little training in vertebrate anatomy can navigate through the embryo in order to locate other features of interest in the model or in their own specimens of similar stage. For this, the biologist first finds the plane of section through the reference embryo that best corresponds to that through his or her own material. This is done by identifying parts of major structures cut by the same section in the specimen and using these structures in the model to interactively define the corresponding plane. With this plane set, the model can be digitally resectioned, if necessary, slightly adjusting the section planes in different parts of the embryo. Comparison of section views with views of whole components and their 3-D relationships can then provide a framework for detailed examination of the users own sections. A similar approach can be used to help interpret whole-mount preparations, matching a volume-rendered view of the model with the conventional view of the specimen under a dissecting microscope. Using the painted anatomical components as landmarks in volume rendered view or in digital sections, the different structures in the specimen embryo can be explored.

Copyright © 1999 by Academic Press. All rights of reproduction in any form reserved.

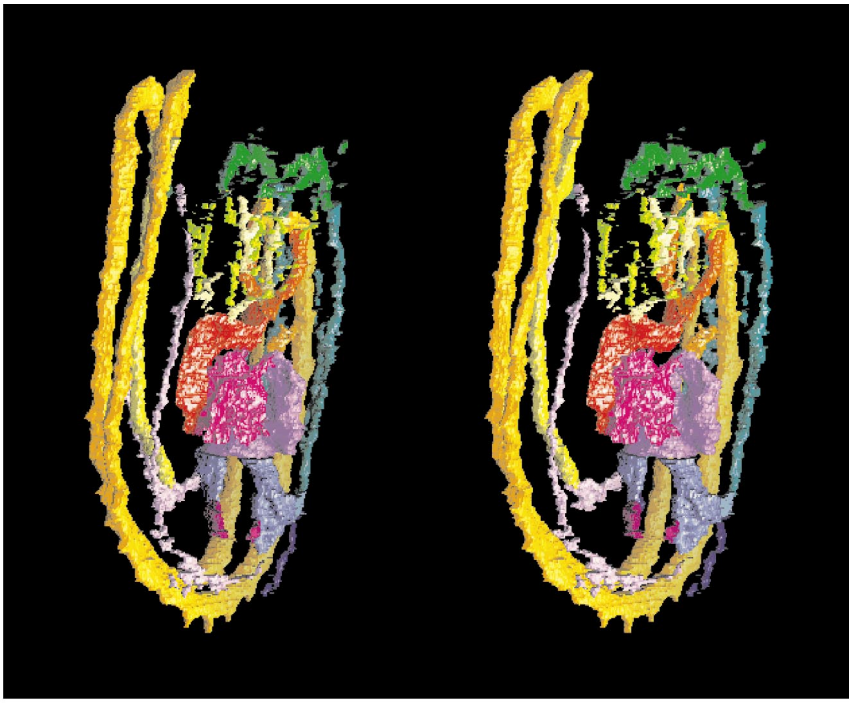

6

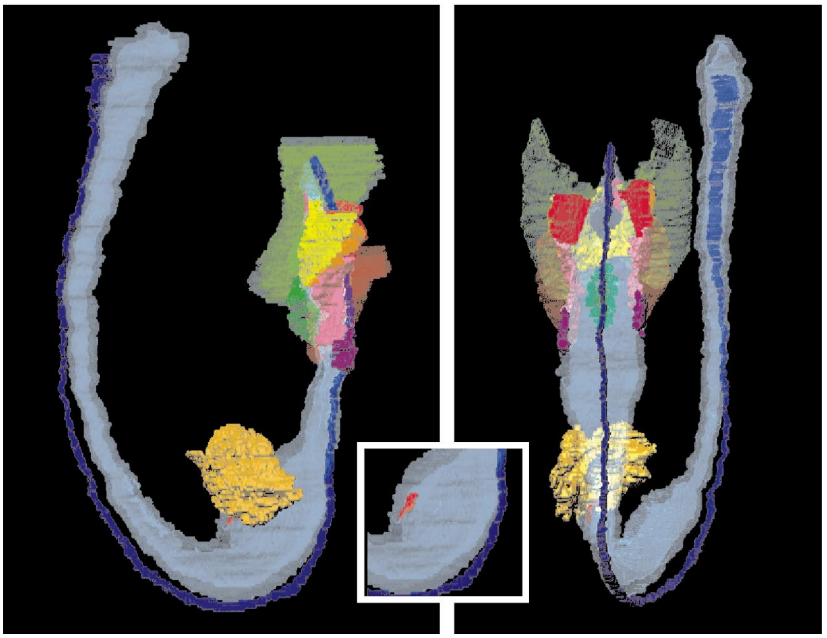

7

FIG. 6. Stereo pair view of the vascular system of the E9 embryo set for "parallel gaze." First arch artery (orange), second arch artery (light orange), dorsal aorta (yellow), vitelline artery (lemon yellow), umbilical artery (dark green), internal carotid artery (cream), vessels connecting internal carotid artery to primary head veins (lime green), primary head veins (dark green), anterior cardinal vein (dark turquoise), common cardinal vein (light blue), posterior cardinal vein (dark blue), umbilical vein (pink), vitelline vein (purple), sinus venosus (lavender blue), common atrial chamber (lilac), primitive ventricle (magenta), and outflow tract (red).

FIG. 7. Gut (transparent blue) with notochord (dark blue), septum transversum (golden yellow), biliary bud (red), mesenchyme of first arch (transparent light green) and second arch (transparent red), branchial pouch of the first arch (solid red) and second arch (purple), lining of the first arch (yellow) and second arch (lilac), endodermal component of first branchial membrane (orange), thyroid primordium (green), and endodermal component of buccopharyngeal membrane (pink). The inset shows the hepatic diverticulum with the biliary bud without the septum transversum.

Copyright © 1999 by Academic Press. All rights of reproduction in any form reserved.

TABLE 1
List of Painted Components in the E9 Embryo

Branchial arch	First arch	Ectoderm	
		Endoderm	
		Mesenchyme	
		First branchial membrane	Ectoderm + endoderm
		Branchial pouch	
	Second arch	Ectoderm	
		Endoderm	
		Mesenchyme	
		Branchial pouch	
Cavities and their linings	Intraembryonic coelom	Pericardial component	Cavity
			Mesothelial lining
		Pericardio–peritoneal canal	Cavity
			Mesothelial lining
		Peritoneal component	Cavity
			Mesothelial lining
Ectoderm	Surface ectoderm		
	Rathke's pouch		
Mesenchyme	Head	Mesenchyme	
		Facioacoustic neural crest	
		Trigeminal neural crest	
		Somites 1–5	
	Body	Mesenchyme	
		Intermediate mesoderm	
		Lateral mesenchyme	Somatopleure
			Splanchnopleure
		Somites 6–18	
		Paraxial mesenchyme	
		Septum transversum	
Notochord			
Organ system	Cardiovascular system—Arteries	First arch artery	
		Second arch artery	
		Dorsal aorta	Left + right
		Internal carotid artery	Left + right
		Umbilical artery	
		Vitelline artery	
	Cardiovascular system—Heart	Common atrial chamber	Cardiac jelly
			Endothelium
			Myocardium
		Primitive ventricle	Cardiac jelly
			Endothelium
			Myocardium
		Outflow tract (includes bulbus cordis)	Cardiac jelly
			Endothelium
			Myocardium
		Sinus venosus	Left horn + right horn
		Mesentery	Dorsal mesocardium
	Cardiovascular system—Veins	Cardinal vein	Anterior
			Common
			Posterior
		Primary head veins	
		Umbilical vein	Left + right
		Vitelline vein	Left + right
	Cardiovascular system—Capillaries	Vessels connecting int. car. to head veins	
	Nervous system	Future brain	
		Future spinal cord	
		Neural lumen	
	Sensory organ	Ear–inner ear	Otic pit
		Eye	Optic vesicle
	Visceral organ	Gut	Gut lumen
			Thyroid primordium
			Biliary bud
		Buccopharyngeal membrane	Ectoderm + endoderm
		Urogenital system	Nephrogenic chord
			Presumptive nephric duct
Primitive streak			
Extraembryonic tissue			

Landmarks that are particularly useful in this context are:

- Rostral tips of foregut and notochord;
- Notochord (as a midline landmark);
- Tip of Rathke's pouch;
- Caudal tip of optic vesicles;
- Edges of otic pit/placode;
- Buccopharyngeal membrane (if present);
- First branchial membrane;
- Rostral tips of primitive ventricle and common atrial chamber;
- Caudal tip of bulbus cordis;
- Bulboventricular groove; and
- Biliary bud.

The cardiovascular system. Figures 5 and 6 show the developing heart and cardiovascular system and illustrate features of the anatomy that are hard to discern in sectioned material. For example, Fig. 6 shows that the rostral part of the vascular system is more developed than the caudal part and that the seventh intersegmental arteries (between somites) that will form the axial arteries to the forelimb are no more extensive than the others. The posterior cardinal vein displays minimal evidence of differentiation compared to the anterior cardinal vein that is now bifurcating into the vessels destined to become the internal and external jugular veins. There is well-defined trabeculation throughout the primitive ventricle and the lesser degree of trabeculation associated with the wall of the bulbus cordis is consistent with its future role as the precursor of the right ventricle and proximal part of the outflow tract.

The primitive gut, the branchial arches, and the septum transversum. Figure 7 shows the primitive gut with the remnants of the buccopharyngeal membrane, the first and second branchial arch pouches, the first branchial membrane, the thyroid primordium, the septum transversum, and biliary bud. The rostral tip of the foregut is seen to have a sharp point that broadens caudally with dorsal-to-ventral flattening. There is one feature that was unexpected and may be an artifact: within the diverticulum, there is a small, hollow globular structure some 50 μm in diameter adjacent to the bud (Figs. 3e and 3f).

Neural tissue. Figure 5c shows a view of the neural tube in combination with the somites, intermediate mesenchyme, optic vesicles, and the heart, all within translucent surface epithelium. The optic vesicles point in a posterosuperolateral direction (like "horns") and five rhombomeres are visible. It should also be noted that there is no clear external morphological demarcation between the caudal part of the future hindbrain and the most rostral part of the future spinal cord. For this model we define this border between the fourth and the fifth somite as shown in Fig. 5c. In addition, the facioacoustic and trigeminal neural-crest-derived preganglionic condensations are first clearly seen at this stage (Figs. 3a and 3b). The notochord has a sharp rostral boundary dorsal to Rathke's pouch, but its caudal boundary is ill defined as its tissue merges into the primitive streak at the caudal part of the embryo (Figs. 5c, 7a, and 7b).

Urogenital tissue. The partitioning of intermediate mesoderm into the nephric cord (kidney precursor tissue) and the nephric duct has only just started at this stage. Figure 5c shows these tissues, together with the somites within the translucent ectoderm. There is asymmetry between the left and right sides. On the left side, the subdivision of the intermediate mesoderm into nephrogenic tissue (medially) and pronephric duct (laterally) occurs at the level of somite 13. On the right side, however, it occurs almost one somite's length more caudally, at the level of somite 14. At the caudal end of the embryo, however, there are no differences between the axial levels of the right and left rudiments and these levels coincide with the caudal level of somite 17.

Size. One additional set of data that can readily be extracted from the reconstruction is the relative volumes of the different anatomical tissues (Table 2). Even allowing for any fixation artifacts in this single embryo, some clear observations can be made. Although the largest single differentiated tissue is clearly the neural tissue (19%), it is obvious that a large volume of the embryo unambiguously derives from the mesoderm (53%), some of which has clearly started to differentiate, e.g., intermediate mesoderm, somites, heart, and vascular system. Nevertheless, 58% of the mesenchyme at this stage still seem undifferentiated, although its fate may already have been determined. What is perhaps surprising is how little of the tissue can be seen as being derived from endoderm: the gut, its largest derivative by far, occupies less than 3% of the tissue.

DISCUSSION

The reconstruction described here shows that it is possible to make a detailed 3-D digital model of the Theiler stage 14 embryo and indicates how it can be used to elucidate information about anatomy not readily obtainable using conventional approaches. It provides an accessible reference description of the E9 embryo, to which developmental data of any sort can be related and in which both the histological and the anatomical structure can be displayed in a view that matches the individual investigator's material. The model can assist structure identification in the embryo; indeed, the delineated anatomical domains in the model provide a definition of the terms used in the anatomical nomenclature database.

The model embryo uniquely provides a view of the stained histological structure of a single embryo that can be explored in three dimensions and so provides a powerful tool to investigate morphogenesis. The ability to demonstrate discrete anatomical domains in isolation, in combination with other tissues, or within a transparent image of the entire embryo can greatly assist us in understanding various relationships between anatomical components. For example, the relationship between the somites and the

Copyright © 1999 by Academic Press. All rights of reproduction in any form reserved.

TABLE 2
Tissue Volumes (Total Volume of Embryo Approximately 0.5 mm^3)

Tissue name	Tissue volume (% whole embryo)	Tissue volume (% of larger component)
Tissues derived from ectoderm	25	
Tissues derived from mesoderm	52	
Tissues derived from endoderm	2.8	
Body cavities	18	
Gut lumen		15
Intraembryonic coelom		50
Neural lumen		34
Otic lumen		1
Heart (incl. lumen)	7.4	
Blood vessels	8.6	
Venous		39
Arterial		61
Central nervous system	18	
Future brain		68
Future spinal cord		32
Central nervous system plus optic vesicles	19	
Urogenital system	0.2	
First branchial arch (incl. artery + blood)	4.2	
Second branchial arch (incl. artery + blood)	1.0	
Total gut	2.8	
Mesenchyme	31	
Head		44
Head somites		2.0
First branchial arch (incl. artery + lumen)		9.4
Second branchial arch (incl. artery + lumen)		2.2
Body		3.9
Body somites		12
Intermediate		2.2
Lateral plate		12
Paraxial		10
Septum transversum		2.3

nephrogenic cords and their ducts can now be seen and fully appreciated for the first time and provide useful landmarks.

In addition to the general features of the anatomy described in this paper, detailed study of the model may reveal further features that have not been detected in unstained whole embryos and have not been apparent from studies of serial, stained sections viewed individually. The combined use of this model with those of younger and older embryos can be expected to provide novel insight into morphogenetic processes and the changing spatial relationships between structures during mouse development. In addition, and within the limitations discussed below, the model provides a reference against which to analyze the phenotypes of, for example, mutant embryos at the appropriate stage of development.

This reconstruction incorporates all the major anatomical features for its stage of development, but if any tissue needs to be further subdivided, or changed, this can be readily incorporated into the model. Once the graphical gene-expression database is established and key gene-expression patterns are mapped, we anticipate that the classical morphological anatomy in the present version of the model will be complemented by a molecular anatomy. This will not only help us to perceive the development of underlying mechanisms, but will also define new landmark domains in the embryo.

There is one further advantage to this reconstruction that is worth mentioning. As the various anatomical components of this typical E9 mouse embryo are very similar to those present in the Carnegie stage 11 human embryo, it is possible, with little difficulty, to use this mouse reconstruction to help study serial sections of human embryos at this stage (usefulness for navigation is limited to the early stages).

Limitations of the Model

The most important limitation of the model is that it is based on a single embryo. It can thus only represent one moment during the interval defined by E9 and gives no

Copyright © 1999 by Academic Press. All rights of reproduction in any form reserved.

indication of the variation in morphology, or any heterochrony, in the development of different organ systems that might be found in a population of the same strain or between different strains. The model and the associated database can however be used as a baseline description for such data.

Similarly, care must be exercised in attempting to use the model in any detailed morphometric analysis, for example, as a standard against which to detect subtle changes of shape in an embryo carrying a mutation. It would be difficult to justify the use of any standard model for such an analysis since artifacts arising from differences in fixation and histological processing confound the comparison. For such a purpose, comparisons would normally be made between numbers of wild-type and mutant embryos processed in parallel. Once these differences have been determined by such a method, the results could, however, be *recorded* in the present model, for example, by delineating the normal structures affected by the mutant phenotype and, perhaps, attaching original images of the mutant phenotype or other data to the appropriate domain. This approach would permit the construction of a searchable database of mutant phenotype and allow them to be compared with gene-expression patterns similarly mapped onto the reference model.

Our choice of specimen also dictates, in part, the resolution of the model, determined by the thickness of the histological sections. For models of early embryos, during gastrulation and the formation of the first few somites, we have used material processed specifically for this work, with a nominal section thickness of 2 μm, which allows a resolution that distinguishes most individual cells in the embryo. The use of an equivalent resolution for the E9 embryo would require a much larger image which would severely reduce the potential for interactive viewing. In the future, models of selected organs (special systems) at higher resolution may be constructed as necessary and embedded within the framework of the whole embryo model. For the present, we intend to make available images of the full series of the original histological sections on which the reconstruction was based. These images will have a pixel size 1.36 $\times$ 1.36 μm and will thus provide a higher resolution at any position in the model.

CONCLUSION

We are making this detailed description widely available and hope that those with an interest in particular developing systems can begin to incorporate this information into their research and, perhaps, comment to us on its uses and limitations. Where appropriate, information (attributed) may be added to the model so that any investigator can retrieve it.

This model is part of a series, which will form the framework for a WWW-based, graphical gene-expression database (Davidson *et al.*, 1997). At present, however, research workers using UNIX workstations can use the model as an aid to investigating the deployment of three-dimensional gene expression in the E9 embryo using the prototype MAPaint program. This can be used immediately for 3-D analysis and for storing simple, or partial, gene-expression patterns in preparation for later entry into the database. Details of how to obtain a copy of the model and MAPaint can be found on the Mouse Atlas WWW site, http://genex.hgu.mrc.ac.uk/. This site also details the current status of WWW-based software for accessing, mapping, and analyzing gene-expression patterns and the graphical gene-expression database.

APPENDIX

Voxel Model Reconstruction

The key requirement of the reconstruction process is to produce a voxel model that is representative of the E9 mouse embryo that can be used for resectioning and with structures visible using standard histological staining. Additionally we want the model to be close to the existing *de facto* standard (Kaufman, 1992). We therefore have developed a reconstruction technique that allows the model to be built from the full set of 307 serial sections, some of which were used in the paper atlas. The parts of the process were digitization, image alignment, image warping, and restacking, to form a 3-D gray-level digital model. All stages of this process use proprietary software and hardware systems developed at the MRC Human Genetics Unit and based on the woolz image processing system (Piper and Rutovitz, 1986).

Image Capture and Alignment

A digital image of each section was recorded using a Zeiss Axioplan microscope fitted with a 5$\times$ Neofluor objective lens and a Xillix 1400 (Optimum Vision Ltd., Petersfield, Hampshire, UK) digital camera linked to a Sun Microsystems Sparc 10. The Xillix camera provides a digital image with a 12-bit gray value (values 0–4095) for each pixel which was converted to 8 bit (values 0–255) and then shade corrected in the usual way (Baldock and Poole, 1993) to remove the effects of uneven illumination and camera sensitivity.

The sections used from the "Atlas of Mouse Development" (Kaufman, 1992) were cut without any fiducial markers; therefore, during capture, the image of each histological section was aligned by using a transparent overlay of the preceding section image in the series. This process produced a stack of registered images ready for the process of warping, which corrects any small registration errors as well as distortions arising from the sectioning process. The stack of images was reviewed using the MRC "Reconstruct" software to correct relative registration errors and to replace bad sections with adjacent ones. The overall 3-D

Copyright © 1999 by Academic Press. All rights of reproduction in any form reserved.

shape of the embryo was checked by viewing the coronal and sagittal sections in MAPaint and adjusting as required.

Warping

Sectioning and histological processing introduce both systematic and random distortions to each section which must be corrected if arbitrary sectioning through the model embryo is to generate a realistic image of a section. A key development for this project has been the production of warping software to correct such random distortions (Guest, 1994; Guest and Baldock, 1996) by modeling each original section image as a thin elastic plate. The basic assumption is that the biological structures visible within the gray-level images are smooth on the scale of the section thickness. In digital image terms, this implies that, if a given point on a tissue section is connected by a straight line in 3-D to the corresponding point in the section above and similarly to the section below, then the two lines will be nearly parallel, i.e., there are no sharp corners. Each section is modeled as a thin elastic plate and linked to the two adjacent sections by "springs" defined by an automatic matching process. The springs deform the sections to smooth out tissue boundaries and the elastic properties of each plate resist excessive deformation so that the original embryo shape is retained. The entire process is fully automatic.

Subsampling

The original 2-D images of successive sections are composed of 1.36×1.36 μm pixels the depth of the voxels in the volume image is the thickness of the sections, i.e., 7 μm. To minimize interpolation when resectioning at an arbitrary orientation, the voxel array should be isotropic. On a cubic lattice the best option would be to have isodiametric voxels, i.e., $7 \times 7 \times 7$ μm. We have compromised by resizing to $4 \times 4 \times 7$ μm: this allowed the retention of adequate resolution without significantly affecting the appearance of the resectioned model. For visualization, the voxels are scaled to give a uniform magnification (although the underlying resolution cannot of course be changed). After warping, Gaussian subsampling (Gaussian smoothing followed by subsampling: Koenderink, 1984) was used to reduce the resolution by a factor of three in each direction in the original planes.

ACKNOWLEDGMENTS

The authors thank Professor Peter Holland and Dr. David Wilkinson for helpful discussions on the head–body division. BBSRC and MRC grants funded part of this work.

REFERENCES

Baldock, R. A., Bard, J. B. L, Kaufman, M. H., and Davidson, D. R. (1992). A real mouse for your computer. *BioEssays* **14,** 501–502.

Baldock, R. A., and Poole, I. (1993). Video camera calibration for optical densometry. *J. Microsc.* **172,** 49–54.

Bard, J., Kaufman, M. H., Dubreuil, C. H., Brune, R. M., Burger, A., Baldock, R. A., and Davidson, D. R. (1998). An internet-accessible database of mouse developmental anatomy based on a systematic nomenclature. *Mech. Dev.* **74,** 111–120.

Davidson, D., and Baldock, R. A. (1997). A 3-D atlas and gene expression database of mouse development: Implications for a database of human development. *In* "Molecular Genetics of Early Human Development" (T. Strachan, S. Lindsay, and D. Wilson, Eds.), pp. 239–260. BIOS, Oxford.

Davidson, D., Bard, J., Brune, R., Burger, A., Dubreuil, C., Hill, W., Kaufman, M., Quinn, J., Stark, M., and Baldock, R. (1997). The mouse atlas and graphical gene-expression database. *Semin. Cell Dev. Biol.* **8,** 509–517.

Guest, E. (1994). "Automatic Reconstruction for Serial Sections," Ph.D. thesis. Department of Artificial Intelligence, University of Edinburgh.

Guest, E., and Baldock, R. A. (1996). Automatic reconstruction of serial sections using the finite element method. *Bioimaging* **3,** 154–167.

Kaufman, M. H. (1992). "The Atlas of Mouse Development." Academic Press, London.

Kaufman, M. H., Brune, R. M., Baldock, R. A., Bard, J. B. L., and Davidson, D. (1996). Computer-aided 3-D reconstruction of serially-sectioned mouse embryos: Its use in integrating anatomical organisation. *Int. J. Dev. Biol.* **41,** 223–233.

Koenderink, J. J. (1984). The structure of images. *Biol. Cybernet.* **50,** 363–370.

Piper, J., and Rutovitz, D. (1986). Data structures for image processing in a C language and unix environment. *Pattern Recog. Lett.* **3,** 119–129.

Ringwald, M., Baldock, R. A., Bard, J. B. L., Kaufman, M. H., Eppig, J. T., Richardson, J. E., Nadeau, J. H., and Davidson, D. R. (1994). A database for mouse development. *Science* **265,** 2033–2034.

Rugh, R. (1968) "The Mouse: Its Reproduction and Development." Burgess, Minneapolis. [reprinted 1990, Oxford Univ. Press, Oxford]

Schroeder, W., Martin, K., and Lorenson, B. (1998). "The Visualization Toolkit," 2nd ed. Prentice Hall International, Englewood Cliffs, NJ.

Theiler, K. (1972). "The House Mouse: Development and Normal Stages from Fertilization to 4 Weeks of Age." Springer Verlag, Berlin.

Theiler, K. (1989). "The House Mouse: Atlas of Embryonic Development." Springer Verlag, New York.

Received for publication March 10, 1999
Revised September 8, 1999
Accepted September 8, 1999

Copyright © 1999 by Academic Press. All rights of reproduction in any form reserved.